

## Physical properties of $\text{TiO}_2$ prepared by sol-gel under different pH conditions for photocatalysis

M. A. Santana-Aranda\*, M. Morán-Pineda, J. Hernández, S. Castillo  
Instituto Mexicano del Petróleo, Ingeniería Molecular-FQG  
Eje Central Lázaro Cárdenas #152 México, D.F. 07730 México

R. Gomez

Universidad Autónoma Metropolitana-Iztapalapa, Depto. Química  
Av. Atlixco #186, México, D.F. 09340 México

(Recibido: 18 de diciembre de 2004; Aceptado: 26 de febrero de 2005)

We present the characterization of the physical properties of titanium dioxide powders prepared by the Sol-Gel method. We set the gelling pH to values of 3 ( $\text{TiO}_2$ -A), 7 ( $\text{TiO}_2$ -N) and 9 ( $\text{TiO}_2$ -B) to observe its effect on the properties of the material. In the three cases we obtained nanoparticulated materials with particle sizes between 10 nm and 20 nm. The larger surface areas were obtained at pH 3, which is several times larger than the other synthesized materials. Furthermore, with the gelling condition pH 3, it was possible to synthesize pure anatase phase titania. We present some preliminary results on the test of photocatalytic activity of the synthesized materials in the reduction of nitric oxide.

**Keywords:**  $\text{TiO}_2$ ; Titanium dioxide; Titania, Sol-gel; Nanoparticles; Photocatalysis

Presentamos la caracterización de las propiedades físicas de polvos de dióxido de titanio preparados por el método de Sol-Gel. Fijamos el pH de gelación en los valores de 3 ( $\text{TiO}_2$ -A), 7 ( $\text{TiO}_2$ -N) y 9 ( $\text{TiO}_2$ -B) para observar su efecto sobre las propiedades del material. En los tres casos obtuvimos materiales nanoparticulados con tamaños de partícula entre 10 y 20 nm. Las áreas superficiales más grandes fueron obtenidas a pH 3, las cuales son varias veces mayores que las de los otros materiales sintetizados. Adicionalmente, con la condición de gelación pH 3, fue posible sintetizar titania con fase anatasa pura. Presentamos algunos resultados preliminares de la prueba de actividad fotocatalítica de los materiales sintetizados en la reducción de óxido nítrico.

**Palabras clave:**  $\text{TiO}_2$ ; Dioxido de titanio; Titania; Sol-gel; Nanopartículas; Fotocatálisis

### 1. Introduction

Titanium dioxide is a semiconductor material with a wide variety of applications; ranging from catalysis and dye sensitized solar cells to cosmetics. Among other factors, this variety of applications of titanium dioxide is possible because of properties like high stability, low cost and non-toxicity [1-3]. Catalytic applications of titanium dioxide have been studied during decades for the elimination of environmental pollutants. Particularly, in the last years  $\text{TiO}_2$  has been studied for photocatalytic processes regarding degradation of pollutants in air, water and soil [4-10]. Currently, synthesis of  $\text{TiO}_2$  by sol-gel methods has proven to be a very useful tool for photoinduced molecular reactions to take place on titanium dioxide surface [11]. There are special variables that affect the photoinduced reactions such as particle size, phase composition, incident light and preparation method; for instance, anatase  $\text{TiO}_2$  nanoparticles has shown higher photocatalytic activity than rutile  $\text{TiO}_2$  [12].

In this work we present results on the characterization of the physical properties of sol-gel synthesized  $\text{TiO}_2$ . We present the effect of the gelling pH on the crystalline phase and particle size and results of the photocatalytic reduction of nitric oxide.

### 2. Experimental details

Titanium dioxide nanoparticles were prepared from titanium alkoxide in 2-propanol (J.T. Baker 9000-03) and distilled water. The hydrolysis of the alkoxide was carried out at different pH values, adjusted by the addition of ammonium hydroxide ( $\text{NH}_4\text{OH}$ ) or hydrochloric acid (HCl). The acidity-alkalinity of the gel were adjusted to the values pH 9 ( $\text{TiO}_2$ -B), pH 3 ( $\text{TiO}_2$ -A) and pH 7 ( $\text{TiO}_2$ -N); additionally, we employed P25 Degussa titanium dioxide as reference material ( $\text{TiO}_2$ -R). Calcination of the synthesized materials was carried out in air at 500 °C during 6 hours in a Fischer Scientific furnace.

Specific surface areas were determined performing BET measurements with a Micromeritics ASAP-2000 apparatus. Particle size determination was carried out with a transmission electron microscope (TEM), JEOL 100CX STEM. The x ray diffraction (XRD) patterns were obtained with a SIEMENS 500 diffractometer. Surface hydroxyls were observed by diffuse reflectance infrared Fourier transform spectroscopy (DRIFTS) using a Nicolet Protégé 460 spectrometer and by x-ray photoelectron spectroscopy (XPS) in a VG ESCALAB 250 spectrometer. Diffuse reflectance spectroscopy measurements in the UV-visible region were employed to determine the band gap energy of the samples. The test for photocatalytic activity in the reduction of nitric oxide was performed by FTIR

\*Corresponding Author: [msantana@ccip.udg.mx](mailto:msantana@ccip.udg.mx)

Current Address: Departamento de Física, CUCEI – Universidad de Guadalajara. Tel/Fax: +52 (33) 3345-4147

**Table 1.** Crystalline phase, specific surface areas, pore volume, average particle sizes, relative OH intensity (XPS), energy band gap and photocatalytic activity of the studied materials.

Sample	Crystalline Phase	Surface Area (m <sup>2</sup> /g)	Pore Volume (cm <sup>3</sup> /g)	Average Particle Diameter (Å)	Relative Intensity O(1s) [OH/TiO <sub>2</sub> ]	Band gap Energy (eV)	NO reduction in 3 hrs (%)
TiO <sub>2</sub> -R	a + r	53.6	0.135	32	-	3.25	25
TiO <sub>2</sub> -A	a	80.8	0.187	12	6.19	3.37	100
TiO <sub>2</sub> -N	a + r	8.7	0.028	20	3.17	3.37	25
TiO <sub>2</sub> -B	a + r	11.2	0.041	19	-	3.49	0

measurements in a Bruker IFS 66v/S spectrometer employing a home made 20 cm length gas cell with a fixed volume.

### 3. Results and discussion

The obtained values for the specific surface area and pore volume of the synthesized materials, as well as the reference material are summarized in table I. As can be seen in this table, we achieved a specific surface area almost 50% higher than that of reference material (TiO<sub>2</sub>-R) in the case of an acid preparation (TiO<sub>2</sub>-A). On the other hand, samples TiO<sub>2</sub>-N and TiO<sub>2</sub>-B have surface areas which are also higher than that of TiO<sub>2</sub>-R; for about 20%. Transmission electron microphotographs (TEM) of the four samples are shown in figure 1. It can be seen in figure 1 that sample TiO<sub>2</sub>-A has the smaller particle sizes; it has well defined granules like the reference sample. On the opposite, samples TiO<sub>2</sub>-N and TiO<sub>2</sub>-B look like agglomerates of small particles slightly bigger than those of the acid sample. Despite this agglomeration, it can be observed that these samples have smaller particle sizes than the reference sample. Average particle sizes are presented in table I. As shown, we have successfully synthesized nanoparticulated titanium dioxide, with average particle sizes smaller or equal to 20 nm.

In figure 2 we show the x ray diffraction (XRD) patterns of the four samples in the 2θ range from 20 to 45 degrees. In this range we can observe, four diffraction peaks of the anatase phase of titania and two peaks of its rutile phase; these peaks are labeled "a" and "r", respectively. XRD results show that the acid preparation consists of pure anatase phase; unlike the reference material, consistent of a mixture of anatase and rutile structures. Like the reference material, the neutral preparation consists of a mixture of anatase and rutile phases. Meanwhile, the material prepared at pH 9 seems to be also pure anatase since its diffraction pattern barely shows evidence of the rutile phase. However, a ten time's magnification of the most intense peak of the rutile phase, inserted in figure 2, unveils the presence of rutile titanium dioxide in this sample. These results indicate that we can synthesize titanium dioxide

with pure anatase phase on will, by adjusting the gelling pH.

The hydroxyl species adsorbed at the surface of the studied samples has been monitored by x ray photoelectron spectroscopy (XPS) and diffuse reflectance infrared Fourier transform spectroscopy (DRIFTS) measurements. The XPS spectra of samples TiO<sub>2</sub>-A and TiO<sub>2</sub>-N are shown in figure 3; the shown ranges are those originated from oxygen 1s and titanium 2p orbitals. The two peaks of titanium 2p ( $\frac{1}{2}$ ,  $\frac{3}{2}$ ) orbitals correspond to the titanium dioxide chemical environment. On the other hand, the peak of oxygen 1s also corresponds to oxygen in titanium dioxide. Furthermore, there is a small shoulder at the left side of the titanium dioxide's oxygen 1s peak; this shoulder is related with hydroxyl species bound to titanium dioxide [13-15]. The differences on the intensity ratio of this shoulder to the principal peak of the different samples give an estimate of the amount of hydroxyl species relative to each other. The intensity ratio values of samples TiO<sub>2</sub>-A and TiO<sub>2</sub>-N are shown in table II, showing a larger amount of hydroxyls in the neutral preparation of titanium dioxide. The DRIFTS spectra of the synthesized materials are shown in figure 4. We observe some differences between the three samples; frequency position and intensity. Hydroxyls band of the acid prepared sample is around 3620 cm<sup>-1</sup>, while in the case of neutral and basic preparation it appears an extra band which is around 3700 cm<sup>-1</sup>. Furthermore, the intensity of the hydroxyl band in the case of the neutral and basic preparations is higher than in the case of the acid preparation. This is in agreement with the results obtained in the analysis of XPS measurements. This relative determination of the amount of hydroxyls is relevant because it has been reported to play an important role in photocatalytic processes [15].

Diffuse reflectance measurements in the UV-visible region allowed us to determine the band gap energy of the samples. The spectral dependence of the absorption coefficient ( $\alpha$ ) of a material is given by the spectral dependence of the absorbance ( $\alpha \sim A$ ). Besides, if we assume a direct band gap of both crystalline phases of titanium dioxide [16], we can express the absorption coefficient with the following formula  $\alpha h\nu \propto (h\nu - E_g)^{\frac{1}{2}}$

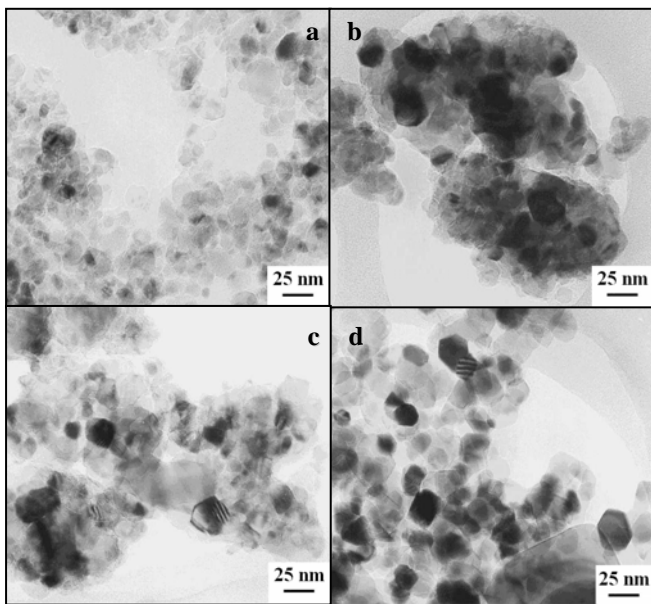


Figure 1. TEM photographs of the studied samples; a)  $\text{TiO}_2$ -R; b)  $\text{TiO}_2$ -A; c)  $\text{TiO}_2$ -N; d)  $\text{TiO}_2$ -B. Reference bar corresponds to 25 nm.

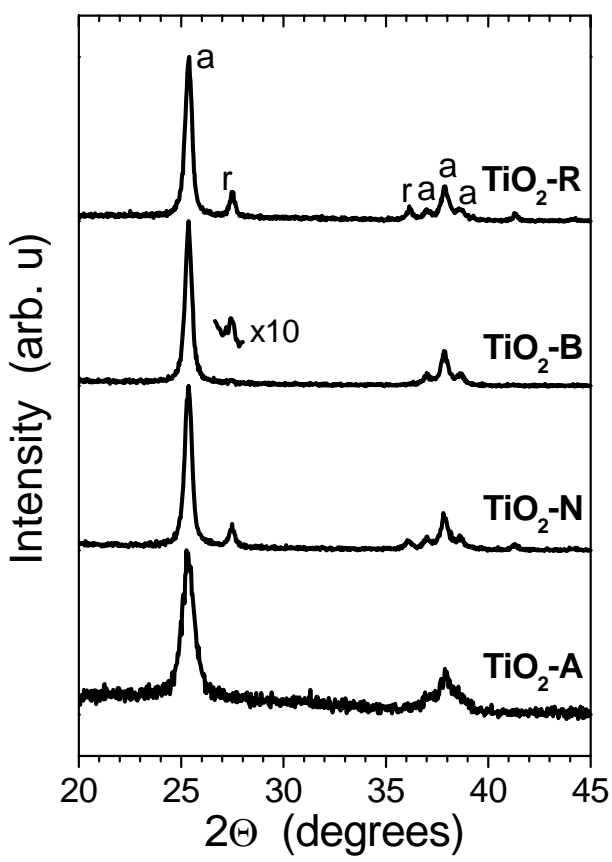


Figure 2. X ray diffraction patterns of studied samples. The patterns are normalized and vertically displaced for clarity. Sample name and diffraction peak phase labels are given.

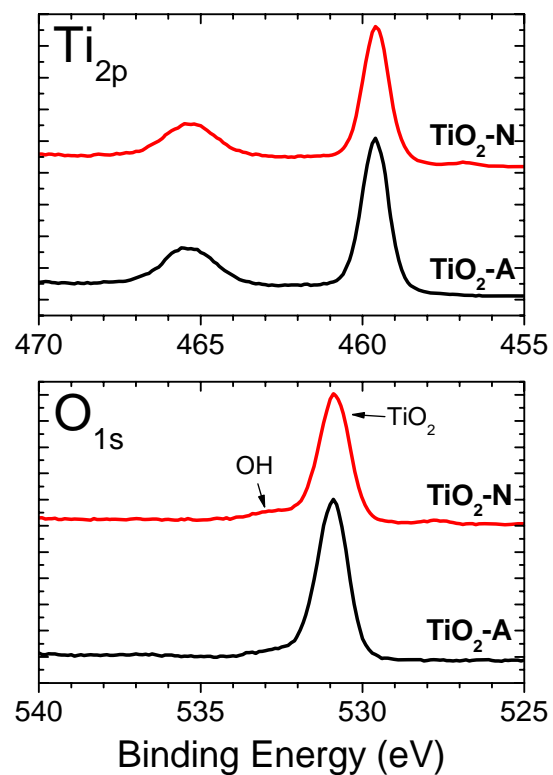


Figure 3. X ray photoelectron spectroscopy measurements of samples  $\text{TiO}_2$ -A and  $\text{TiO}_2$ -N in the regions of  $\text{Ti}(2p)$  and  $\text{O}(1s)$  orbitals.

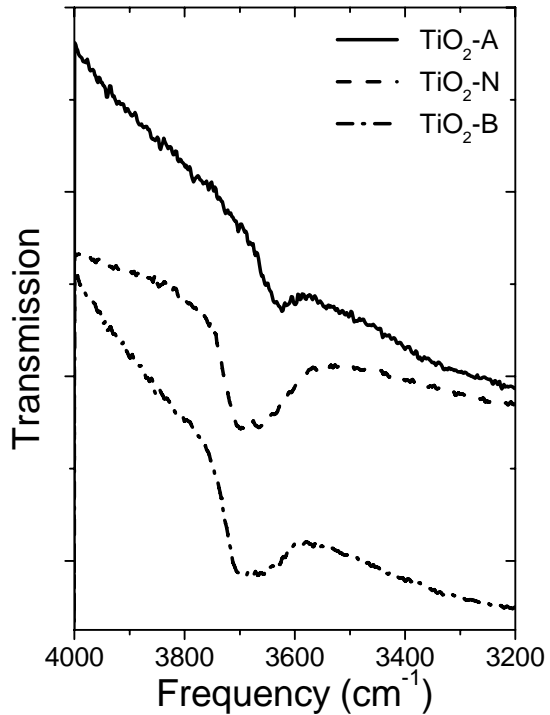


Figure 4. Infrared transmission spectra obtained from DRIFTS measurements, in the region of the absorption band of hydroxyl species.

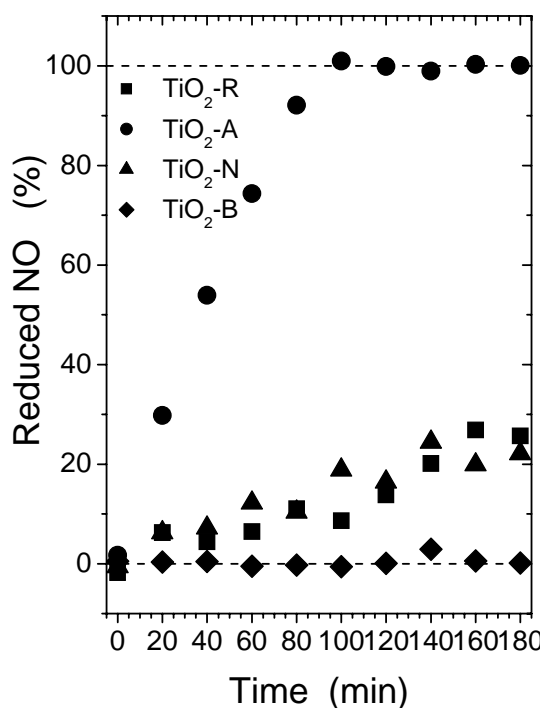


Figure 5. Profile of the percent of nitric oxide reduced monitored during 180 minutes of light exposure for photocatalytic evaluation.

as a function of the band gap energy ( $E_g$ ) and the energy of the incident photon ( $h\nu$ ). Therefore, the band gap energy can be determined by extrapolation to the energy axis of the linear interval in a plot  $(\alpha h\nu)^2$  vs.  $h\nu$ . The band gap energy values obtained in this way for the reference and synthesized materials are summarized in Table I. As can be seen, in Table I, the band gap energy of the studied materials keep the following order  $E_g(R) < E_g(A) = E_g(N) < E_g(B)$ . This order in the energy band gap values does not keep a relation with the reactivity observed for the set of samples.

The test for photocatalytic activity carried on for nitric oxide reduction was monitored during 180 minutes (3 hours) and is shown in figure 5. It shows the decomposition percentage of the nitric oxide loaded into the reaction cell as a function of illumination time. As can be observed in this figure, we succeeded in the preparation of titanium dioxide with reactivity for the photocatalytic reduction of nitric oxide. It can be observed that sample  $\text{TiO}_2\text{-A}$  is the one with the highest reactivity for the photocatalytic reduction of nitric oxide. It takes 100 minutes under illumination for sample  $\text{TiO}_2\text{-A}$  to reduce the concentration of nitric oxide below noise level. Meanwhile, samples  $\text{TiO}_2\text{-N}$  and  $\text{TiO}_2\text{-R}$  have a slower reactivity, eliminating only about 20% of the nitric oxide during the 3 hours period shown in fig. 5. On the other hand, sample  $\text{TiO}_2\text{-B}$  is clearly deficient with no evident decomposition of NO during the monitored time interval. We found no conclusive evidence for energy band gap or hydroxyl content influence on the photocatalytic reactivity. The higher reactivity seems to be mostly related to the pure anatase phase of the sample and secondly with the

nanometric size of the particles. These two properties have been previously pointed out as important factors for photocatalytic reactions by other authors [17, 18]. Further work is under way to study in more detail the photocatalytic activity of the synthesized materials.

#### 4. Conclusions

We have successfully synthesized nanoparticulated titanium dioxide with particle sizes between 12 nm and 20 nm. We also obtained pure anatase titanium dioxide by adjusting the gelling pH to a value of pH 3. This pH condition also leads to a surface area of  $80 \text{ m}^2/\text{g}$ , which is 50% higher than that of the commercial sample material. The test for photocatalytic activity showed that our synthesized materials have similar and even better photocatalytic reactivity than the reference material employed.

#### Acknowledgments

Authors want to thank R. Velázquez Lara for technical assistance and the Instituto Mexicano del Petróleo (IMP) for financial support. One of the authors (MASA) is indebted to the IMP for a postdoctoral fellowship.

#### References

- [1] G. Colón, M.C. Hidalgo, J.A. Navío, *Appl. Catal. A* **231**, 185(2002).
- [2] K.M. Reddy, S.V. Manorama, A.R. Reddy, *Mater. Chem. Phys.* **78**, 239(2002).
- [3] J.G. Yu, J.C. Yu, B. Cheng, S.K. Hark, K. Iu, *J. Sol. State Chem.* **174**, 372(2003).
- [4] J. Zhang, T. Ayusawa, M. Minagawa, K. Kinugawa, H. Yamashita, M. Matsuoka, M. Anpo, *J. Catal.* **198**, 1(2001).
- [5] D.S. Bhatkhande, V.G. Pangarkar, A.A.C.M. Beenackers, *J. Chem. Technol. Biot.* **77**, 102(2002).
- [6] S. Malato, J. Blanco, A. Vidal, D. Alarcon, M.I. Maldonado, J. Caceres, W. Gernjak, *Solar Energy* **75**, 329(2003).
- [7] N.L. Stock, J. Peller, K. Vinodgopal, P.V. Kamat, *Environ. Sci. Technol.* **34**, 1747(2000).
- [8] L.B. Khalil, M.W. Rophael, W.E. Mourad, *Appl. Catal. B-Environ.* **36**, 125(2002).
- [9] M.M. Higarashi, W.E. Jardim, *Catal. Today* **76**, 201(2002).
- [10] J. Zhao, X.D. Yang, *Building and Environ.* **38**, 645(2003).
- [11] H.D. Jang, S.K. Kim, S.J. Kim, *J. Nanopart. Res.* **3**, 141(2001).
- [12] Scaflani, L. Palmisano, M. Schiavello, *J. Phys. Chem.* **94**, 829(1990).
- [13] Y.F. Gao, Y. Masuda, Z.F. Peng, T. Yonezawa, K. Koumoto, *J. Mater. Chem.* **13**, 608(2003).
- [14] J.C. Yu, L.Z. Zhang, Z. Zheng, J.C. Zhao, *Chem. Mater.* **15**, 2280(2003).
- [15] L.Q. Jing, X.J. Sun, W.M. Cai, Z.L. Xu, Y.G. Du, H.G. Fu, *J. Phys. Chem. Solids* **64**, 615(2003).
- [16] S.D. Mo, W.Y. Ching, *Phys. Rev. B* **51**, 13023(1995).
- [17] L. Cao, Z. Gao, S.L. Suib, T.N. Obee, S.O. Hay, J.D. Freihaut, *J. Catal.* **196**, 253(2000).
- [18] A.J. Maira, J.M. Coronado, V. Augugliaro, K.L. Yeung, J.C. Conesa, J. Soria, *J. Catal.* **202**, 413(2001).